

Localization and propagation analysis of ictal source rhythm by electrocorticography

June Sic Kim^a, Chang Hwan Im^b, Young Jin Jung^b, Eun Young Kim^{a,1}, Sang Kun Lee^c, Chun Kee Chung^{a,*}

^a MEG Center, Department of Neurosurgery, Seoul National University College of Medicine, Seoul, South Korea

^b Department of Biomedical Engineering, Yonsei University, Wonju, South Korea

^c Department of Neurology, Seoul National University College of Medicine, Seoul, South Korea

ARTICLE INFO

Article history:

Received 17 November 2009

Revised 9 February 2010

Accepted 18 April 2010

Available online 24 April 2010

Keywords:

Ictal onset zone

Source localization

Propagation

Electrocorticography

Directed transfer function

Monte-Carlo simulation

Epilepsy

ABSTRACT

The purpose of this study was to develop a novel approach for objectively estimating the locations of ictal onset zones by electrocorticography (ECoG). Conventional ECoG analyses have been performed using a 2-D space comprised of intracranial electrodes. Thus, despite the fact that ECoG data have much higher signal-to-noise ratios than electroencephalographic data, ECoG inherently requires a priori information to locate the electrodes, and thus, it is difficult to estimate the depth of epileptogenic foci using this technique. Accordingly, the authors considered that a 3-D approach is needed to determine the presence of an epileptogenic focus in the complex structure of the cortex. However, no source localization procedure has been devised to determine the location of a primary ictal source using ECoG. The authors utilized a spatiotemporal source localization technique using the first principal vectors. A directed transfer function was then employed for the time series of potential ictal sources to compute their causal inter-relationships, from which the primary sources responsible for ictal onset could be localized. Monte-Carlo simulation studies were performed to validate the feasibility and reliability of the proposed ECoG source localization technique, and the obtained results demonstrated that the mean of localization errors with a signal to white Gaussian noise ratio of 5 dB did not exceed 5 mm, even when the source was located ~20 mm away from the nearest electrode. This validated ictal source localization approach was applied to a number of ictal ECoG data sets from six successfully operated epilepsy patients. The resultant 3-D ictal source locations were found to coincide with surgical resection areas and with traditional 2-D electrode-based source estimates. The authors believe that this proposed ECoG-based ictal source localization method will be found useful, especially when ictal sources are located in a deep sulcus or beyond recording planes.

© 2010 Elsevier Inc. All rights reserved.

Introduction

Despite recent advances in neuroimaging techniques used for the non-invasive presurgical evaluation of epilepsy, ictal electrocorticography (ECoG) is still considered the gold standard for identifying epileptogenic foci (Engel et al., 1981). However, the interpretation of ictal ECoG recordings is highly dependent on investigator experience and familiarity with the technique, due to the presence of artifacts and a variety of abnormal patterns (Arroyo et al., 1993). The conventional approaches used to determine the locations of epileptogenic foci are based on the use of intracranial electrodes, which depict the first activation on a two-dimensional sensor sheet. The first electrode site to show ictal activity in intracranial recordings often corresponds to the region of maximal epileptogenicity, and amplitude differences are

manually mapped on grid figures to define the phase reversal of maximal discharges (Alarcon et al., 1997; Sutherland and Barth, 1989). Furthermore, topographic mapping using ictal ECoG discharges provides a quantitative means of identifying ictal onset zones (Otsubo et al., 2001).

The value of conventional ECoG diagnosis is controversial in both lesional and nonlesional epilepsies. In lesional epilepsy, the seizure-free rate has been reported to be 19% in 30 patients with a temporal mass lesion treated by lesionectomy alone, but 93% in patients that undergo electrophysiologically guided resection (Zooma et al., 1995). However, ECoG might not be necessary for determining surgical resection area in the case of extratemporal glioma lesions (Fried, 1995). Another study also reported good surgical outcomes (a 79% seizure-free rate) after tumor resection, regardless of electrophysiological findings (Morris et al., 1998).

In nonlesional epilepsy, invasive recordings are typically required to define the epileptogenic zone (Lüders and Comair, 2001; Quesney and Niedermeyer, 2005), and ECoG studies have demonstrated the intrinsic value of identifying resectable ictal onset zones (Henry et al., 1999; Jung et al., 1999; Paolicchi et al., 2000). However, it is still difficult to identify epileptogenic points in the sulcus precisely using subdural electrodes.

These shortcomings may arise in part from the inherent limitations of 2-D approaches. *A-priori* information is needed to locate ECoG

* Corresponding author. Department of Neurosurgery, Seoul National University Hospital, 28 Yeongun-dong Jongro-gu, Seoul, 110-744, South Korea. Fax: +82 2 2072 0806.

E-mail address: chung@snu.ac.kr (C.K. Chung).

¹ Current address: Department of Psychology, Yonsei University, 134 Shinchon-dong Seodaemun-gu, Seoul 120-749, South Korea.

electrodes, and it is difficult to estimate the depth of epileptogenic foci from subdural electrode data. Although 2-D electrocortical topographic mapping could be used to identify ictal onset zones because they are associated with high temporal resolution and a fast sampling rate in lesional and nonlesional cases (Yoshida et al., 2007), there is a potential risk of mislocalization when the current direction is other than radial or a lesion is located some distance from electrodes. Accordingly, a 3-D approach in source space is required to avoid selection bias and to identify epileptogenic foci in the complex cortical structure. However, no ECoG-based source localization procedure has been devised for localizing primary sources.

Many patients with epilepsy have consistent seizure onset foci, and the localization of ictal onset zones is more beneficial for surgical planning than for the mapping of complex interictal patterns (Bebin et al., 1993). The localization of epileptogenic foci has been advanced by source localization and imaging techniques based on electroencephalography (EEG) (Michel et al., 1999; Worrell et al., 2000) and magnetoencephalography (MEG) (Assaf et al., 2003), which characterize seizures in source space rather than in sensor space. Ictal source localization methods integrate characteristic information of ictal sources in space, time, and frequency domains. Some methods utilize estimations of discrete spatiotemporal dipoles to identify ictal generators (Assaf and Elbersole, 1997; Boon et al., 2002), and frequency analysis and dipole localization have also been used in combination for this purpose (Lantz et al., 1999). Another approach was devised using the distributed source model to image more distributed seizure sources (Oishi et al., 2006). The majority of previously described methods use time–frequency parameterization of measured data as an initial step. Moreover, since useful signals may be lost during parameterization and it is difficult to determine signals of interest using time–frequency presentations, a spatiotemporal source localization approach was devised that exploits time–frequency parameterization in the source domain instead of measured channels (Ding et al., 2007). Kamiński and Blinowska (1991) utilized the directed transfer function (DTF) to estimate dynamic causal interaction patterns among sources. Furthermore, the DTF technique was found to provide an excellent guide for the localization of primary ictal sources, and was also used to the channel analysis of invasive recordings to two-dimensionally identify seizure onset electrodes and seizure propagation between electrodes (Franaszczuk and Bergey, 1998; Franaszczuk et al., 1994).

Epileptic studies using intracranial electrodes are advantageous for investigating the dynamics of seizure. An example of one such study is provided by an investigation of the dual pathology between the medial and lateral parts of the temporal lobe using subdural and depth electrodes in order to characterize the activity of epileptogenic foci (Fauser and Schulze-Bonhage, 2006). In another recent analysis of seizure dynamics using multichannel ECoG, a generic change was found in the correlation structures of the data (Schindler et al., 2007), namely, that differences between the propagation times of locally synchronous ictal discharges might disrupt correlations between electrodes. Cortico-muscular dynamics during clonic seizures have also been studied (Hammer et al., 2003). In this previous study, using subdural and depth electrodes, focal clonic seizures were generated by localized polyspike-wave activity in cortical primary motor areas; furthermore, the subthalamic nucleus was not found to be an essential component for the generation of clonic seizures. However, these approaches were all based on the use of 2-D ECoG electrodes, and neuronal dynamics at regions of seizure onset could be further analyzed in more detail by identifying causal relationships between 3-D epileptogenic sources.

Source localization and the estimations of causal interactions have not been popular in ECoG, because this modality measures neuronal activity in a field relatively close to the ictal onset zone, and thus, seizure onset zone is identified based on visual comparisons of signals recorded from different electrodes. However, it is difficult to

determine the depths and three-dimensional locations of ictal sources using ECoG alone. Moreover, it may not be possible to place invasive electrodes over the entire area of an epileptogenic zone, and when multiple sources are identified, it is difficult to identify the primary ictal onset source. Therefore, a source analysis procedure is required that determines the primary ictal onset sources by utilizing source localization and propagation analysis in ECoG. Source reconstruction from ECoG data is a relatively new field because only potential maps have been drawn from measurements (Fuchs et al., 2007). In the present study, we evaluated ictal source locations using a spatiotemporal source localization technique and ECoG data. To achieve this, dipole sources were localized using the first principal vectors (FINE) algorithm (Ding and He, 2006), and then causal interactions among sources were estimated to determine the primary ictal onset source. Monte-Carlo simulations were also performed to determine the feasibility of source localization using ECoG.

Materials and methods

Subjects

Six subjects with medically intractable seizures were selected for this retrospective study. All subjects were evaluated for seizure surgery using various modalities, which included intracranial subdural electrode arrays for seizure localization. Three patients had lesional epilepsy, and the other three had non-lesional epilepsy. All patients were seizure-free after surgery (Engel class I) (Engel, 1987). A brief list of the patient demographic data is presented in Table 1. Intracranial recordings were acquired for all patients. During invasive monitoring, subdural strips and grids were tailored for each patient to cover suspicious regions discovered by video EEG monitoring, MEG, magnetic resonance image (MRI), positron emission tomography (PET), and single photon emission computed tomography (SPECT). In all patients, typical seizures were recorded and reviewed by epileptologists. ECoG signals were digitally acquired at a sampling rate of 200 Hz (Telefactor, Grass Technologies).

Preprocessing for ictal source localization

All subjects were scanned using a 3-T MR unit (Signa VH/I; General Electric) with a conventional head gradient coil. MR images were acquired using a regular T1-weighted spoiled gradient recalled (SPGR) sequence for head images. Slices were spaced 1.5 mm apart, and were acquired in the sagittal orientation with a matrix size of 256 by 256. Using scanned MR images, boundary element method (BEM) models and a source space composed of three dimensional uniform grids were extracted using CURRY 5.0 (Neuroscan™). The BEM models consisted of two homogeneous compartments, namely, cerebrospinal fluid (CSF) and gray matter. The inner skull boundary and the interface between CSF and gray matter were tessellated using surface triangular elements. The volume conduction effect outside the inner skull boundary was ignored in this study due to the very low electrical conductivity of the human skull layer (Fuchs et al., 2007).

After inserting grids and strips of electrodes for invasive monitoring, 3-D computed tomography (CT) (Brilliance 64; Philips) was performed to register the electrodes on preoperative MR images. CT slices were spaced 1.00 mm apart, and a matrix size of 512 by 512 was used. The 3-D locations of electrodes, which were expressed as high-density regions in images, were picked up manually. Electrode locations were then co-registered onto individual MRI data. To compensate for electrode pickup errors by CT and co-registration errors, each electrode was attached to the nearest boundary element on the interface between CSF and gray matter. Using the BEM volume conductor model and electrode positions, a lead field electrode matrix was constructed by applying the node-based first order BEM formulation (Moshier et al., 1999).

Table 1
Demography of epilepsy patients.

Patients ID	Age	MRI	Video EEG ^a	Location of intracranial electrodes ^a	Surgery
1	18	Non-lesional	Left T	Right F, T	Right anterior temporal lobectomy with amygdalohippocampectomy
2	33	Non-lesional	Left T	Left T Right F	Right frontal lobectomy
3	34	Tissue loss and cerebromalacia in right posterior temporal lobe	Right T, P	Right P, T, O	Right parieto-occipital lesionectomy
4	28	Right hippocampal sclerosis and posttraumatic leptomenigeal cyst in the right frontal convexity	Right T	Right F, T	Right anterior temporal lobectomy with amygdalohippocampectomy
5	24	Non-lesional	Right T	Right T	Right lateral temporal lobectomy
6	29	Right hippocampal sclerosis and venous anomaly in the left frontal lobe	T (lateralization is not definite)	Right F, T, P Left T	Left anterior temporal lobectomy with amygdalohippocampectomy

^a F, P, T, and O denote frontal, parietal, temporal, and occipital lobes, respectively.

ECoG data were reviewed by an epileptologist. Seizure onset times and electrodes were visually identified. One to three seizures were observed per subject. Fig. 1 demonstrates ECoG waves of the six subjects during ictal onset.

Spatiotemporal source localization

In this study, the FINE algorithm (Ding and He, 2006; Xu et al., 2004) was used to estimate multiple sources from ECoG ictal signals. In brief, this algorithm models equivalent current dipoles by calculating the subspace correlation between dipolar topographies and estimating signal space or noise-only subspace. When an arbitrary source set is written as a linear superposition of point sources, the corresponding set of time dependent signals of the multiple ECoG electrodes, $\Phi(t)$, can be further defined in matrix format as:

$$\Phi(t) = A(L, Q)S(t)$$

where S is the temporal behavior matrix of sources, A is the lead field matrix, L is a set of location vectors, and Q is a set of their associated orientation vectors.

The measurement space is divided into signal and noise-only subspaces by applying singular value decomposition to the measurement data matrix, $\Phi = U\Lambda V^T$. The columns of U consist of p -dimensional signal subspace and $N-p$ -dimensional noise-only subspace, where N is the number of electrodes. At a region θ , a FINE vector set, F_θ , is identified as an intersection set between the noise-only subspace and the array manifold spanned by the specific region θ , using the concept of principal angles (Buckley and Xu, 1990; Golub et al., 1996). The subspace correlation, SC^2 , metric for the FINE algorithm is described as:

$$SC^2(\bar{l}) = \min_{\bar{q}} \bar{q} \left(\frac{A(\bar{l}, \bar{q})^T F_\theta F_\theta^T A(\bar{l}, \bar{q})}{A(\bar{l}, \bar{q})^T A(\bar{l}, \bar{q})} \right)$$

where \bar{l} and \bar{q} indicate the location vectors of L and the associated orientation vectors of Q , respectively.

The FINE algorithm requires a subspace correlation threshold, and any value below this threshold can be regarded as a possible source. We used 10% as the threshold for FINE vectors. It has been previously reported that a greater number of signal vectors does not significantly change determined source locations (Mosher et al., 1992). The locations and orientations of estimated sources were determined by minimizing the scanning metric $SC^2(1)$. In this study, source locations were uniformly distributed at intervals of 5 mm. Using determined multiple dipole locations, L , and the corresponding orientations, Q , a

lead field matrix A was reconstructed for these multi-dipoles. Source waveforms, S , were then computed using $S = A^+ \Phi$, where A^+ indicates the pseudo-inverse solution of A obtained by truncating singular value decomposition.

Error simulation of ECoG source localization according to depth and deviation

Monte-Carlo simulation studies were performed to test the feasibility and reliability of the proposed ECoG source localization method. Simulation tests included two types of dipole sources. Type-I tests were used to simulate dipoles under electrodes and to estimate the degree of error according to the depth of sources. This simulation is of central importance to the validation of the ECoG source analysis method, since one advantage of the method is to identify ictal locations in folded sulci. Type-II tests were used to simulate dipoles outside the region covered by electrodes and to estimate the degree of error according to the distance from the boundary of the electrodes. ECoG suffers from selective bias with respect to the placement of electrodes, since they do not cover the entire brain, and if an epileptogenic focus is located slightly outside the electrodes, the conventional topographic method could mislocalize the ictal onset zone.

Source activity from a dipole location with an arbitrary orientation was transformed into activity of electrodes using a lead field matrix, and white Gaussian noise was added to transformed signals. In the present study, a signal-to-noise ratio (SNR) of 5 dB was used. To simulate actual data, up to 5 multiple concurrently active sources were randomly generated. To evaluate the fitting accuracy of multiple sources, pairs of simulated and estimated sources were determined using closest distances. Sources estimated using the FINE algorithm were then compared to simulated locations. In the FINE algorithm, the number of dipoles during estimation was the same as the number of dipoles during simulation. This procedure was repeated using 10,000 randomly generated sources with different locations and orientations.

Ictal source propagation

Multiple dipoles were estimated by source analysis. This section introduces a method for determining the primary epileptogenic source from multiple dipole sources. The Directional Transfer Function (DTF) approach was used to analyze ictal source propagation. This function is formulated in the framework of the multivariate autoregressive (MVAR) model, and is well described in the literature (Babiloni et al., 2005; Ding et al., 2007; Kamiński and Blinowska, 1991). Accordingly, to the MVAR model, a multivariate process can be

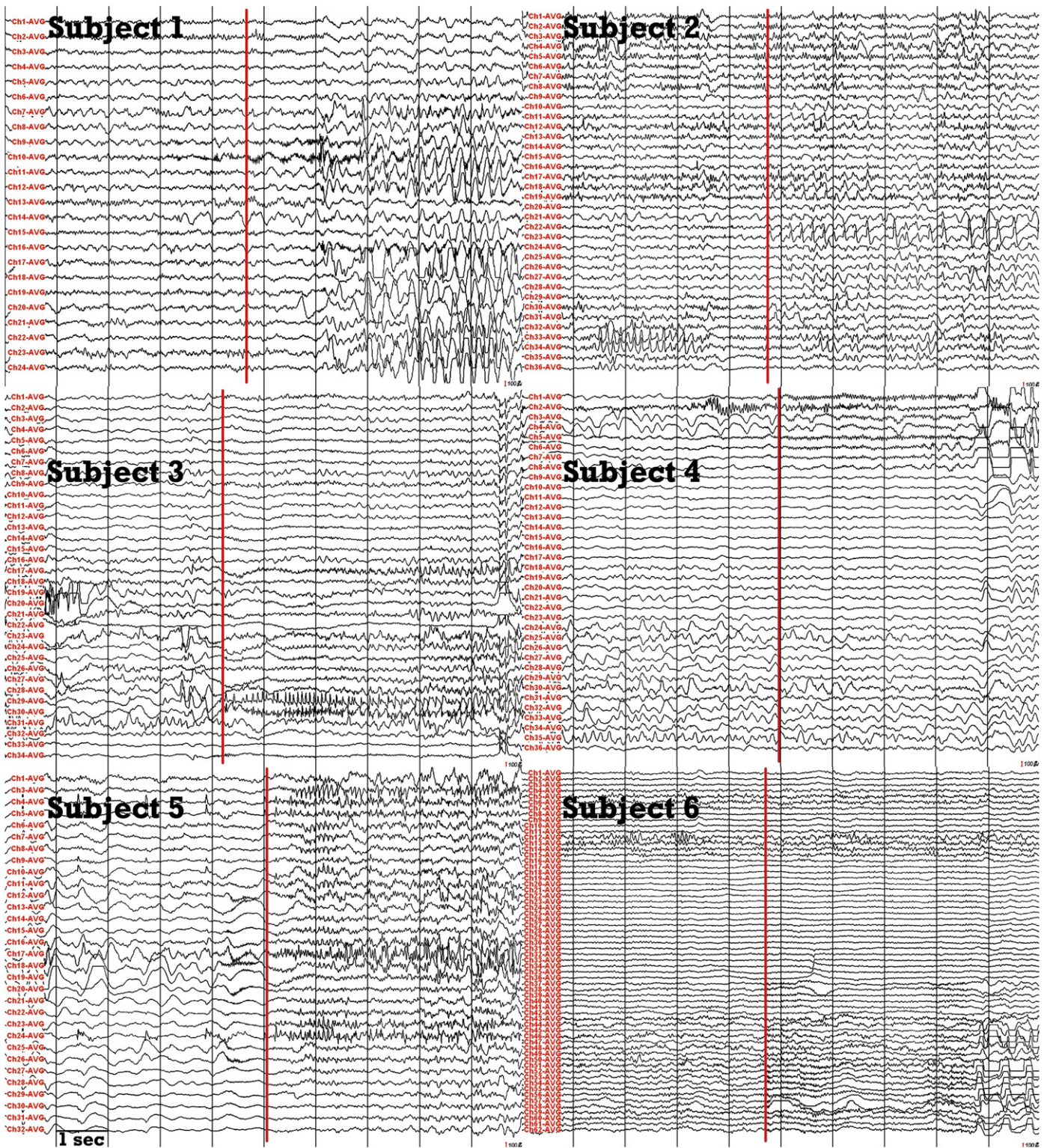


Fig. 1. The ECoG waves of six subjects at around ictal onset. The duration of the recording shown above was 10 s. The red line indicates the time of onset, as determined by an epileptologist.

described as a data vector S of M source signals, estimated as described in Spatiotemporal source localization, in time: $S(t) = (S_1(t), S_2(t), \dots, S_M(t))^T$. The MVAR model can then be constructed as:

$$S(t) = \sum_{n=1}^p P(n)S(t-n) + E(t)$$

where $E(t)$ is the vector of white noise values at time t , P_n is an $M \times M$ matrix comprised of the model coefficients, and p is the model order.

In the present study, model order was determined using criteria derived from Akaike's information criterion (AIC) (Akaike, 1974). Model orders between 1 and 10 were chosen. Individual model orders from subject 1 to 6 are 5, 7, 3, 2, 3, and 4, respectively.

The MVAR model was transformed into the frequency domain as follows:

$$S(f) = P^{-1}(f)E(f) = H(f)E(f)$$

where f denotes frequency and $P(f) = -\sum_{n=0}^p P(n)e^{-i2\pi fn\Delta t}$ with $P(0) = -I$ (I is the identity matrix). $H = P^{-1}$ is inverse of the coefficient matrix P in the frequency domain. The $H(f)$ matrix is the so-called transfer matrix of the system.

The DTF was defined in terms of the elements of the transfer matrix H_{ij} as:

$$\gamma_{ij}^2(f) = \frac{|H_{ij}(f)|^2}{\sum_{m=1}^M |H_{im}(f)|^2 + \varepsilon}$$

where $\gamma_{ij}(f)$ denotes the ratios between inflows from sources j to i to all inflows of activity to the destination source i . ε is added to the denominator to prevent from dividing by very small numbers, which may lead exaggerated DTF values in the normalization. And ε is determined by $0.0001 * \max\left(\sum_{m=1}^M |H_{im}(f)|^2\right)$ where the maximum is taken over frequency variable.

Such DTF ratio takes values from 0 to 1. Values close to 1 indicate that most of the signal in source i is caused by the signal from source j . On the other hand, values close to 0 indicate that there is no information flow from source j to i at a particular frequency. Although the DTF can examine any range of frequencies, a frequency band of 1–70 Hz was used to maintain consistency.

DTF requires at least weak stationary data. Data during long time may not be stationary although rhythmic waves dominate during the ictal period. We tested propagation using the DTF with a time window

of 1 sec. This time window started at seizure onset, which is determined by an epileptologist. In this study, we used only one window for each ictal event.

Statistical evaluation using surrogate signals

The distribution of DTF estimators is not well established because DTF functions have a highly nonlinear relationship with time series data. So, we employed a non-parametric statistical estimation method. A surrogate data technique was used to test the significance of propagation between activities (Kamiński et al., 2001; Theiler et al., 1992). Conceptually, propagation among sources is destroyed when source signals are randomly ordered in time. The surrogate technique randomly and independently shuffles time series data from each source to create a surrogate data set. In order to shuffle time series data, we randomized phases in the Fourier transformed signal so as to leave the power spectra of source signals intact. Propagation was then derived from this surrogate data set. By performing this process many times (10,000 times in the present study), we were able to create an empirical distribution for a given estimator. These distributions provided null hypotheses, since the randomly generated surrogate data set contained no interaction between sources. For example, if there were three source activities, six propagation results among sources are estimated by DTF analysis. Then six empirical distributions for multiple propagation pairs were also generated using the surrogate approach. Thus, significant levels for multiple pairs were determined from each empirical distribution. In the present study, a mean value of multiple frequencies as well as individual frequencies from 1 Hz to 70 Hz was used to reconstruct empirical distributions. The significance level at each frequency is shown as a blue line in Fig. 3. And the significance of each directional pair is shown as red bars in Fig. 3.

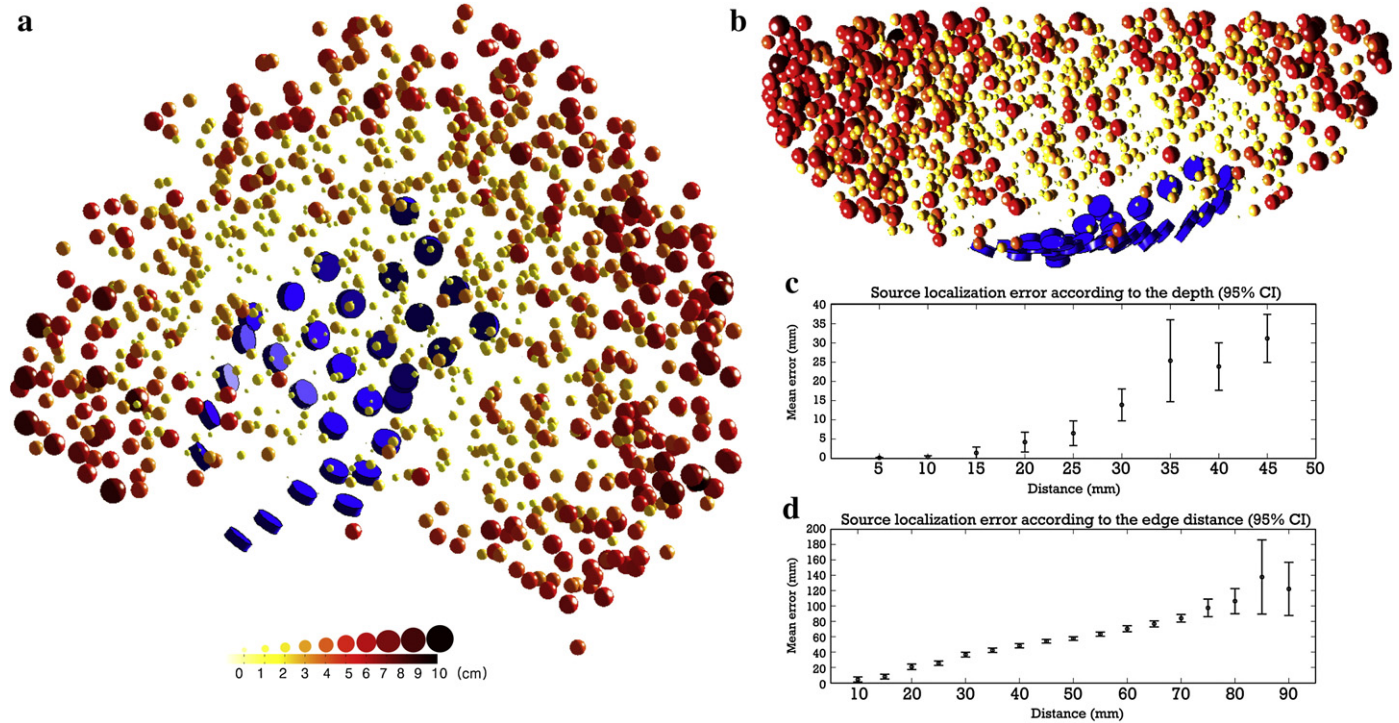


Fig. 2. Localization errors between 10,000 simulated dipole sources and sources estimated using the FINE algorithm. (a) The 3-D error distribution is depicted by disk colors and sizes in lateral view and (b) in top view. Blue disks denote intracranial electrodes. Large localization errors are large and brightly colored. The localization errors at each simulated location along the (c) depth and (d) distance from the boundary of electrodes set are shown separately. Error means and standard deviations increased with respect to depth and distance from the boundary of electrodes set.

Results

Localization errors of simulated data

Localization errors at different distances from the boundary of the electrodes set are shown in Fig. 2. Fig. 2(a) and (b) demonstrate the three-dimensional error distribution in lateral and top views, respectively, and shows that localization error increases with distance from the nearest electrode. When dipole sources are located inside and outside the perpendicular boundary of the electrodes set, localization errors with respect to depth and boundary distance are estimated, respectively. Fig. 2(c) and (d) display errors with respect to depth (b) and distance from the boundary of the electrodes set (c), respectively. Simulated sources were distributed from 5 to 50 mm beneath (b) and from 10 to 95 mm outside (c) electrodes. In both cases, localization errors increased as the distance between source and electrodes increased. However, despite the low SNR of 5 dB, the mean localization error was only 4.18 mm at a source location 20 mm beneath the electrodes, and the mean localization error was ~8.06 mm at a source location 15 mm outside the electrodes. Accordingly, localization error was found to increase substantially with distance outside electrodes.

Ictal source localization and propagation analysis

We evaluated the qualities of dipolar fits using the FINE algorithm using percent variance unexplained (PVU). The PVUs of subject 1 to 6 were 0.210, 0.1713, 0.1075, 0.0198, 0.277, and 0.1756, respectively, and distances from the closest electrode were 11 mm, 23 mm, 5 mm, 9 mm, 7 mm, and 15 mm, respectively. Ictal sources localized using the FINE algorithm and interactions between sources are shown in Fig. 3. The primary onset source was identified by estimating propagation between sources. To determine the significances of propagations, 10,000 surrogate signals were generated. The DTF distributions were then reconstructed using DTF values of each frequency in the range 1 to 70 Hz. Finally, a DTF significance level of $P=0.01$ was determined in each frequency. This threshold level ($P=0.01$) at each frequency was represented as a blue line in Fig. 3. In order to determine significant propagation pairs, mean DTF values in the range of 1 to 70 Hz were also tested with 10,000 surrogate signals. And the significant pairs were displayed as red bars in Fig. 3 even though DTF values were not significant in all frequency ranges. In Fig. 3, DTF distributions were sorted in descending dipole strength order. Note that the most significant emanative source did not have the strongest dipole. Even the smallest dipole could have been the primary ictal onset source in subjects 1 and 6. In all subjects, the ictal onset source determined by propagation analysis was found to be located well inside the surgical resection area. Ictal sources, identified by the proposed method, were compared to conventional ECoG diagnosis (Fig. 4). An epileptologist reviewed ECoG signals at ictal onset times, and determined which electrodes showed rhythmic ictal onset activity. The sources identified were agreed well with conventional ECoG results in most cases, except in subject 2. In this subject, the estimated ictal onset source was surrounded by both ictal onset electrodes and electrodes interictal activity. During surgery, the region enclosing both the ictal and interictal pathologic electrodes was resected.

Evaluation of surgical outcome

Follow-up periods ranged from 18 to 24 months (mean, 20.5 months) postoperatively. All patients benefited from surgery and achieved an excellent seizure outcome (Engel class I). Ictal onset sources estimated by source localization and DTF analysis well matched resection regions in all patients.

Discussion

In the present study, we evaluated a method derived from the directed transfer function technique to identify ictal rhythm by ECoG and epileptogenic foci. A beneficial surgical outcome depends on accurate epileptogenic zone delineation, while avoiding eloquent areas. This approach combines source localization and propagation measures between ECoG ictal sources. Furthermore, dynamic patterns between ictal sources were found to distinguish primary sources of ictal activity from secondary sources caused by propagation from primary ictal sources. Our simulation test results and comparisons with surgical outcomes suggest that the devised technique is feasible for clinical use.

Source localization and simulation testing

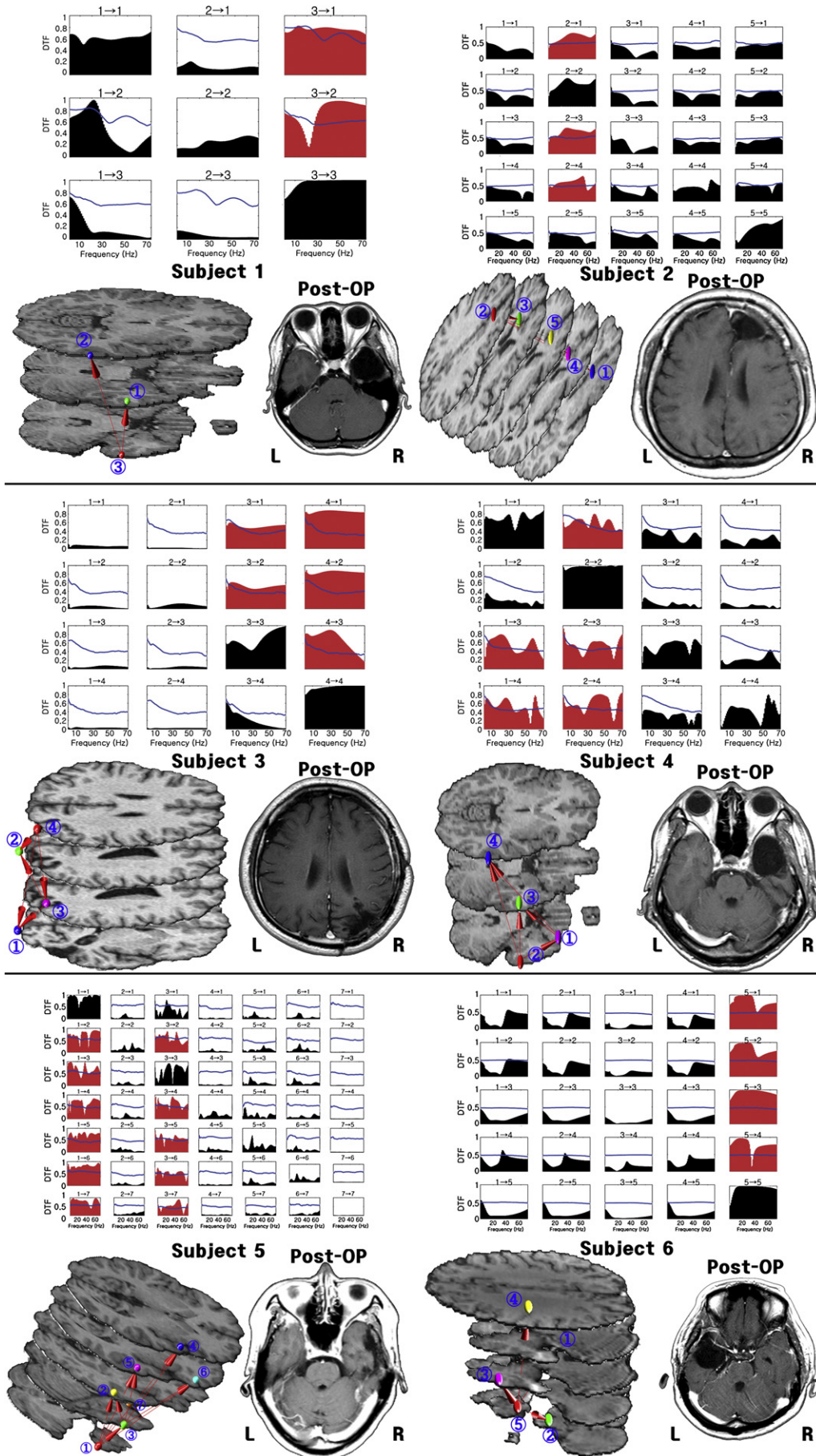
Monte-Carlo simulation was used to evaluate the source localization technique for ECoG data. In simulations without registration or electrode location errors, the accuracy of ECoG source localization largely depends on distances from the electrodes and the depth of sources. The primary cause of inaccuracy at far distance may be due to the inability of the grid electrodes to cover the full extent of the electric field pattern. Using a limited distance range of 8 cm from electrodes, the simulation test revealed small localization errors of 4 mm at 20 mm away from the electrodes along the depth. However, additional errors may arise in practice, for example, those associated with electrode site locations. We assumed that electric potentials were recorded at the centroid of the electrode geometry. However, the actual recording electrolyte interface and double ion layer are more complex, and thus, the actual location of a sensor site may be more difficult to determine. This type of error could also arise during CT to MR image registration.

The *a priori* assumptions that are implemented during the localization procedure determine the localization results. There is an ongoing debate regarding the validity of these *a priori* assumptions and the comparative properties of algorithms. Although systematic evaluations and comparisons of different inverse solutions were not performed in the present study, Monte-Carlo simulations were used to evaluate the validity of the FINE algorithm used to evaluate ECoG data. In addition, source activity within 20 mm of electrodes was reliably localized.

Propagation analysis

In the DTF matrix of Fig. 3, the diagonal indicates the power spectra of the signals normalized by subtraction of mean value and division by variance. And the off diagonal elements are directed transfer functions presenting directional information flow between multiple sources. For example, in subject 1, the element of the first row and the third column indicate directional flow from source 3 to source 1. This DTF

Fig. 3. Sources localized using the FINE algorithm and their activity flows estimated using the directed transfer function (DTF) technique for six epilepsy patients. In each subject, DTF values from 1 to 70 Hz are displayed at the top of the figure. Columns and rows are sorted by dipole activity in descending order of dipole strength. Source activities flow from columns to rows. To determine the significance of each propagation result between sources, we used the DTF values of each frequency from 1 to 70 Hz. The significance level of $P=0.01$ at each frequency is marked as a blue line at each DTF result. Although DTF values are not significant in all frequencies, significant propagation pairs are determined by the surrogate test with the mean DTF values in the range of 1 to 70 Hz. Then the significant pairs are shown by red bars. The red bars indicate the overall significance of the propagation for specific pairs.



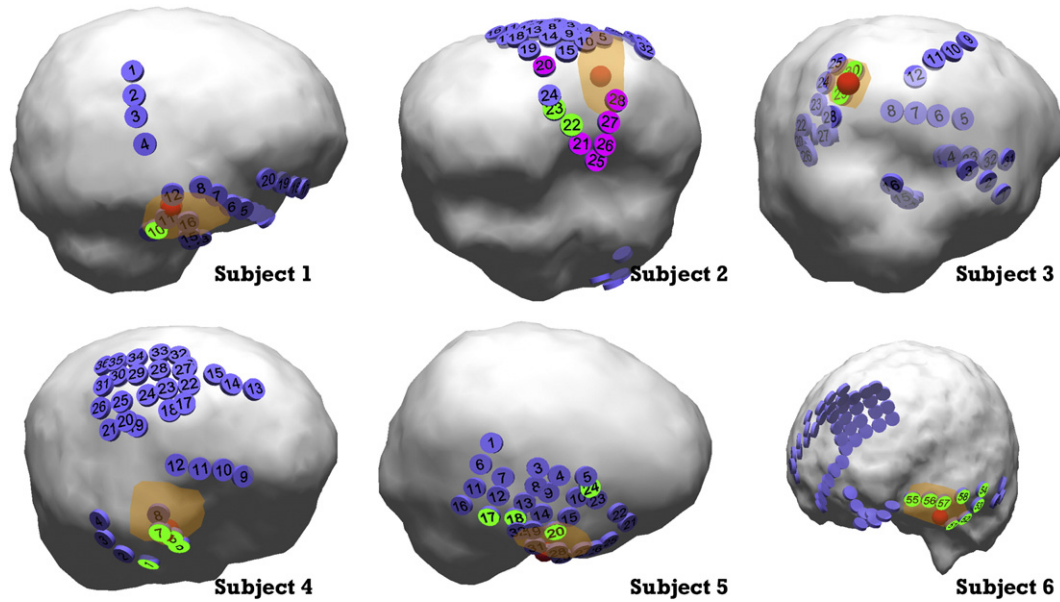


Fig. 4. Comparison between the location of ictal sources estimated using the proposed procedure and conventional ECoG results. Red spheres are ictal onset sources estimated using the FINE algorithm and DTF analysis. Green electrodes denote ictal onset zones determined by an epileptologist. The purple electrodes shown in subject 2 indicate frequent pathologic rhythmic delta activity. Surgical resection areas are colored light orange.

spectrum is high in the whole frequency range. The element of the second row and the third column shows information flow from source 3 to source 2. This DTF spectrum is mainly high in the range of 30 to 70 Hz. Moreover, these two elements are statistically significant by a surrogate test with the mean DTF values. Thus, source 3 can be considered as the primary ictal onset source. In subject 3, DTFs from two sources (No. 3 and No. 4) are significant. However, DTF from source 4 to source 3 is significant mainly at the frequency range of 1 to 50 Hz while DTF from source 3 to source 4 is not. Thus, source 4 can be considered as the primary ictal onset source.

This study provides a reliable means of determining the location of epileptogenic foci using the directed transfer function technique. The problems of determining the directionality of ictal rhythm propagation and of finding causal relationships between brain areas are interesting in the context of identifying epileptogenic foci. It is crucial that we understand information transfer, the sequence in which it is processed, and the roles of specific brain structures during perceptual and cognitive tasks. The devised method locates epileptogenic foci by finding directional interactions between sources identified by ictal rhythm. Source localization using the FINE algorithm could reduce the number of signals for propagation analysis. In addition, conventional ECoG studies have determined the location of ictal onset zones by analyzing sequential differences in amplitudes between electrodes (Miyagi et al., 2005; Otsubo et al., 2001; Yoshida et al., 2007). However, it may be difficult to identify onset zones using rhythmic activity. According to our results, the strongest dipole was not the primary emanative source, except in subject 5. On the other hand, the weakest dipole was possibly the epileptogenic focus in subjects 1 and 6. Small initiating signals can cause larger activities in propagated sources than at the origin if propagated areas are large or have strong neuronal synchronizations.

The DTF technique is based on MVAR, and Granger causality is another popular technique based on MVAR (Granger, 1969). Although Granger causality does not calculate the value of phases in the frequency domain, DTF provides information on the directional and spectral properties of interactions between sources. This technique estimates information flow using a parametric spectrum, and can analyze a data set with a sample size as small as 50 (Astolfi et al., 2007). Furthermore, DTF is robust with respect to noise or constant

phase disturbances (Kamiński and Blinowska, 1991), but the data set required must be obtained from wide-sense stationary processes, since DTF is based on a multivariate autoregressive algorithm. The development or application of new techniques that can accurately measure the directional connectivity between non-stationary time series is crucial for more accurate estimations of ictal propagation patterns.

Clinical cases

In the present study, epileptogenic foci estimated by dipole modeling and propagation analysis corresponded well with the region of successful surgical resection in all subjects. In particular, in subjects 4 and 6, estimated sources were located even in regions around sparsely distributed strip electrodes. In subjects 4 and 6, grid electrodes were installed in the fronto-parietal area, whereas in both cases epileptogenic sources were estimated to be in the temporal lobe. This demonstrates that our approach is able to identify epileptogenic foci using few electrodes. However, when electrodes are sparsely distributed, electric potential field maxima and minima might not be recorded. Therefore, the dipole source model might be limited in terms of its ability to fit the potential pattern as precisely as it does in fully covered regions. However, further study is required to evaluate source modeling under various conditions.

Subject 2 was an interesting case. In most subjects, estimated ictal onset sources were located in a region close to visually identified ictal onset electrodes. However, in subject 2, ECoG electrodes were installed in the right frontal and left temporal lobes, and during an ictal event, rhythmic beta was identified in the posterior portion of the frontal lobe. However, during interictal recording, pathological delta rhythm activity was frequently observed on the strip of electrodes covering the inferior frontal area. Thus, surgery was performed using the electrodes that showed rhythmic delta activity (the purple electrodes in Fig. 4) and ictal beta activity (green electrodes in Fig. 4), but eloquent areas were avoided. The surgical resection area included the anterior frontal region. However, the ictal onset source in this subject was located in the space between grid and strip electrodes, and the source location was far removed from the ictal

onset electrodes. One possible explanation for this difference is that the ictal rhythm was recorded on irrelevant electrodes due to the direction of the dipole source and volume conduction. This limitation could be overcome by using a source approach to identify the primary source.

ECoG ictal rhythm

This integrated technique was previously introduced to analyze EEG ictal rhythm and to localize the epileptogenic focus (Ding et al., 2007). Accordingly, to the results of this earlier study, the results of noninvasive ictal source localization and propagation analysis suggest consistency between EEG-based ictal sources and MRI/SPECT diagnosed sources. However, dipole modeling of ictal EEG activity is difficult mainly because of EEG artifacts, such as, electromyographic artifact, electrode movements, and eye movements, which are often seen during seizures (Gotman, 2003). Despite its invasiveness, ECoG is better than EEG or MEG for localizing ictal onset sources (Engel, 1996; Wyllie et al., 1988), especially, if source analysis of the electrode data can be fully exploited. The present study is the first to propose a source approach to ictal ECoG and its validation. This 3-D source approach is supported by a recent ECoG study, in which a distributed source imaging method was used to identify interictal spikes (Zhang et al., 2008). The results of this recent study, which used simulated data sets and one epilepsy patient, showed that ECoG is superior to scalp EEG as a source imaging technique due to its high signal-to-noise ratio. In contrast to this approach, we used the ictal onset data sets of six patients, and clinically validated the derived 3-D source technique when used in combination with propagation analysis. Furthermore, the present study shows the value of the 3-D approach as compared with the conventional 2-D approach.

Ictal ECoG recordings are considered the gold standard for identifying epileptogenic foci (Stefan et al., 1992; Yoshida et al., 2007). However, the technique devised in the present study has the advantage that it localizes source activities and determines information flow between sources using ECoG ictal data. Many studies have demonstrated the values of MEG and EEG source localizations using interictal spikes to identify seizure foci in temporal and extratemporal lobe epilepsy (Baumgartner et al., 2000b; Iwasaki et al., 2002). Propagated sources may appear on interictal EEG, MEG, or ECoG. However, ictal rhythms are believed to have more localizing value than interictal spikes (Jayakar et al., 1991). Although several MEG and EEG studies have reported consistent interictal and ictal onset localizations (Tang et al., 2003; Wheless et al., 1999), interictal spikes may represent an irritative zone that does not necessarily encompass the ictal focus (Baumgartner et al., 2000a). Further study is required to examine the merits of ECoG for interictal source localization and propagation analysis.

Conclusions

In this study, we originally applied a spatiotemporal source localization technique called FINE to a number of ictal ECoG data sets, and subsequent simulation studies demonstrated the feasibility of ictal source localization using ECoG. Furthermore, propagation analysis using the directed transfer function was found to differentiate ictal onset sources from propagated sources.

Acknowledgments

This research was supported by grants from the Brain Research Center of the 21st Century Frontier Research Program (2009K001280) funded by the Ministry of Education, Science and Technology, the Republic of Korea.

The authors would like to thank Dr. Antti Ahonen and Dr. Ritva Paetau for their valuable comments.

References

- Akaike, H., 1974. A new look at statistical model identification. *IEEE Transactions on Automatic Control* AC-19, pp. 716–723.
- Alarcon, G., Garcia Seoane, J.J., Binnie, C.D., Martin Miguel, M.C., Juler, J., Polkey, C.E., Elwes, R.D., Ortiz Blasco, J.M., 1997. Origin and propagation of interictal discharges in the acute electrocorticogram. Implications for pathophysiology and surgical treatment of temporal lobe epilepsy. *Brain* 120.
- Arroyo, S., Lesser, R.P., Awad, I.A., Goldring, S., Sutherland, W.W., Resnick, T., 1993. Subdural and epidural grids and strips. In: Engel Jr., J. (Ed.), *Surgical Treatment of the Epilepsies*. Raven Press, New York, pp. 377–397.
- Assaf, B.A., Elberse, J.S., 1997. Continuous source imaging of scalp ictal rhythms in temporal lobe epilepsy. *Epilepsia* 38, 1114–1123.
- Assaf, B.A., Karkar, K.M., Laxer, K.D., Garcia, P.A., Austin, E.J., Barbaro, N.M., Arinoff, M.J., 2003. Ictal magnetoencephalography in temporal and extratemporal lobe epilepsy. *Epilepsia* 44, 1320–1327.
- Astolfi, L., Cincotti, F., Mattia, D., Marciani, M.G., Baccala, L.A., de Vico Fallani, F., Salinari, S., Ursino, M., Zavaglia, M., Ding, L., Edgar, J.C., Miller, G.A., He, B., Babiloni, F., 2007. Comparison of different cortical connectivity estimators for high-resolution EEG recordings. *Human Brain Mapping* 28, 143–157.
- Babiloni, F., Cincotti, F., Babiloni, C., Carducci, F., Mattia, D., Astolfi, L., Basilisco, A., Rossini, P.M., Ding, L., Ni, Y., Cheng, J., Christine, K., Sweeney, J., He, B., 2005. Estimation of the cortical functional connectivity with the multimodal integration of high-resolution EEG and fMRI data by directed transfer function. *Neuroimage* 24, 118–131.
- Baumgartner, C., Pataraja, E., Lindinger, G., Deecke, L., 2000a. Magnetoencephalography in focal epilepsy. *Epilepsia* 41, 39–47.
- Baumgartner, C., Pataraja, E., Lindinger, G., Deecke, L., 2000b. Neuromagnetic recordings in temporal lobe epilepsy. *Journal of Clinical Neurophysiology* 17, 177–189.
- Bebin, E.M., Kelly, P.J., Gomez, M.R., 1993. Surgical treatment for epilepsy in cerebral tuberous sclerosis. *Epilepsia* 34, 651–657.
- Boon, P., D'Havé, M., Vanrumste, B., Van Hoey, G., Vonck, K., Van Walleghem, P., Caemaert, J., Achten, E., De Reuck, J., 2002. Ictal source localization in presurgical patients with refractory epilepsy. *Journal of Clinical Neurophysiology* 19, 461–468.
- Buckley, K.M., Xu, X.L., 1990. Spatial-spectrum estimation in a location sector. *IEEE Transactions on Acoustics, Speech, & Signal Processing* 38, 1842–1852.
- Ding, L., He, B., 2006. Spatio-temporal EEG source, localization using a three-dimensional subspace FINE approach in a realistic geometry inhomogeneous head model. *IEEE Transactions of Biomedical Engineering* 53, 1732–1739.
- Ding, L., Worrell, G.A., Lagerlund, T.D., He, B., 2007. Ictal source analysis: localization and imaging of causal interactions in humans. *Neuroimage* 34, 575–586.
- Engel Jr., J., 1987. Outcome with respect to epileptic seizures. In: Engel Jr., J. (Ed.), *Surgical treatment of the epilepsies*. Raven Press, New York.
- Engel Jr., J., 1996. Surgery for seizures. *New England Journal of Medicine* 334, 647–652.
- Engel Jr., J., Rausch, R., Lieb, J.P., Kuhl, D.E., Grandall, P.H., 1981. Correlation of criteria used for localizing epileptic foci in patients considered for surgical therapy of epilepsy. *Annals of Neurology* 9, 215–224.
- Fauser, S., Schulze-Bonhage, A., 2006. Epileptogenicity of cortical dysplasia in temporal lobe dual pathology: an electrophysiological study with invasive recordings. *Brain* 129, 82–95.
- Franaszczuk, P.J., Bergey, G.K., 1998. Application of the directed transfer function method to mesial and lateral onset temporal lobe seizures. *Brain Topography* 11, 13–21.
- Franaszczuk, P.J., Bergey, G.K., Kaminski, M.J., 1994. Analysis of mesial temporal seizure onset and propagation using the directed transfer function method. *Electroencephalography and Clinical Neurophysiology* 91, 413–427.
- Fried, I., 1995. Management of low-grade gliomas: results of resections without electrocorticography. *Clinical Neurosurgery* 42, 453–463.
- Fuchs, M., Wagner, M., Kastner, J., 2007. Development of volume conductor and source models to localize epileptic foci. *Journal of Clinical Neurophysiology* 24, 101–119.
- Golub, G.H., van Loan, C.F., Golub, G.H., van Loan, C.F., 1996. *Matrix computations*, 3rd ed. Johns Hopkins University Press, Baltimore, MD.
- Gotman, J., 2003. Noninvasive methods for evaluating the localization and propagation of epileptic activity. *Epilepsia* 44, 21–29.
- Granger, C.W.J., 1969. Investigating causal relations by econometric models and cross-spectral methods. *Econometrica* 37, 424–438.
- Hammer, H.M., Lüders, H.O., Knake, S., Fritsch, B., Oertel, W.H., Rosenow, F., 2003. Electrophysiology of focal clonic seizures in humans: a study using subdural and depth electrodes. *Brain* 126, 547–555.
- Henry, T., Ross, D.A., Schuh, L.A., Drury, I., 1999. Indications and outcome of ictal recording with intracerebral and subdural electrodes in refractory complex partial seizures. *Journal of Clinical Neurophysiology* 16, 426–438.
- Iwasaki, M., Nakasato, N., Shamoto, H., Nagamatsu, K., Kanno, A., Hatanaka, K., Yoshimoto, T., 2002. Surgical implications of neuromagnetic spike localization in temporal lobe epilepsy. *Epilepsia* 43, 415–424.
- Jayakar, P., Duchowny, M., Resnick, T.J., Alvarez, L.A., 1991. Localization of seizure foci: pitfalls and caveats. *Journal of Clinical Neurophysiology* 8, 414–431.
- Jung, W.Y., Pacia, S.V., Devinsky, O., 1999. Neocortical temporal lobe epilepsy: intracranial EEG features and surgical outcome. *Journal of Clinical Neurophysiology* 16, 419–425.
- Kamiński, M., Blinowska, K., 1991. A new method of the description of the information flow in the brain structures. *Biological Cybernetics* 65, 203–210.
- Kamiński, M., Ding, M., Truccolo, W.A., Bressler, S.L., 2001. Evaluating causal relations in neural systems: Granger causality, directed transfer function and statistical assessment of significance. *Biological Cybernetics* 85, 145–157.

- Lüders, H.O., Comair, Y.G., 2001. Epilepsy surgery, 2nd ed. Lippincott Williams & Wilkins, Philadelphia.
- Lantz, G., Michel, C.M., Seeck, M., Blanke, O., Landis, T., Rosén, I., 1999. Frequency domain EEG source localization of ictal epileptiform activity in patients with partial complex epilepsy of temporal lobe origin. *Clinical Neurophysiology* 110, 176–184.
- Michel, C., Grave De Peralta, R., Lantz, G., Gonzalez Andino, S., Spinelli, L., Blanke, O., Landis, T., Seeck, M., 1999. Spatiotemporal EEG analysis and distributed source estimation in presurgical epilepsy evaluation. *Journal of Clinical Neurophysiology* 16, 239266.
- Miyagi, Y., Morioka, T., Fukui, K., Kawamura, T., Hashiguchi, K., Yoshida, F., Shono, T., Sasaki, T., 2005. Spatio-temporal analysis by voltage topography of ictal electroencephalogram on MR surface anatomy scan for the localization of epileptogenic areas. *Minimally Invasive Neurosurgery* 48, 97–100.
- Morris, H.H., Matkovic, Z., Estes, M.L., Prayson, Y.A., Comair, Y.G., Turnbull, J., Najm, I., Kotagal, P., Wyllie, E., 1998. Ganglioglioma and intractable epilepsy: clinical and neurophysiological features and predictors of outcome after surgery. *Epilepsia* 39, 307–313.
- Mosher, J.C., Lewis, P.S., Leahy, R.M., 1992. Multiple dipole modeling and localization from spatio-temporal MEG data. *IEEE Transactions on Biomedical Engineering* 39, 541–557.
- Mosher, J.C., Leahy, R.M., Lewis, P.S., 1999. EEG and MEG: forward solutions for inverse methods. *IEEE Transactions on Biomedical Engineering* 46, 245–259.
- Oishi, M., Otsubo, H., Iida, K., Suyama, Y., Ochi, A., Weiss, S.K., Xiang, J., Gaetz, W., Cheyne, D., Chuang, S.H., Rutka, J.T., Snead, O.C.R., 2006. Preoperative simulation of intracerebral epileptiform discharges: synthetic aperture magnetometry virtual sensor analysis of interictal magnetoencephalography data. *Journal of Neurosurgery* 105, 41–49.
- Otsubo, H., Shirasawa, A., Chitoku, S., Rutka, J.T., Wilson, S.B., Snead, O.C.R., 2001. Computerized brain-surface voltage topographic mapping for localization of intracranial spikes from electrocorticography. Technical note. *Journal of Neurosurgery* 94, 1005–1009.
- Paolicchi, J.M., Jayakar, P., Dean, P., Yaylali, I., Morrison, G., Prats, A., Resnik, T., Alvarez, L. A., Duchowny, M., 2000. Predictors of outcome in pediatric epilepsy surgery. *Neurology* 54, 642–647.
- Quesney, L.F., Niedermeyer, E., 2005. Electrocorticography. In: Niedermeyer, E., Da Silva, F.L. (Eds.), *Electroencephalography: basic principles, clinical applications and related fields*. Lippincott Williams & Wilkins, Philadelphia.
- Schindler, K., Leung, H., Elger, C.E., Lehnertz, K., 2007. Assessing seizure dynamics by analysing the correlation structure of multichannel intracranial EEG. *Brain* 130, 65–77.
- Stefan, H., Schneider, S., Feistel, H., Pawlik, G., Schüler, P., Abraham-Fuchs, K., Schlegel, T., Neubauer, U., Huk, W.J., 1992. Ictal and interictal activity in partial epilepsy recorded with multichannel magnetoencephalography: Correlation of electroencephalography/electrocorticography, magnetic resonance imaging, single photon emission computed tomography, and positron emission tomography findings. *Epilepsia* 33, 874–887.
- Sutherling, W.W., Barth, D.S., 1989. Neocortical propagation in temporal lobe spike foci on magnetoencephalography and electroencephalography. *Annals of Neurology* 25, 373–381.
- Tang, L., Mantle, M., Ferrari, P., Schifftbauer, H., Rowley, H.A., Barbaro, N.M., Berger, M.S., Roberts, T.P.L., 2003. Consistency of interictal and ictal onset localization using magnetoencephalography in patients with partial epilepsy. *Journal of Neurosurgery* 98, 837–845.
- Theiler, J., Eubank, S., Longtin, A., Galdrikian, B., Farmer, J.D., 1992. Testing for nonlinearity in time series: the method of surrogate data. *Physica D* 58, 77–94.
- Wheless, J.W., Willmore, L.J., Breier, J.I., Katakaki, M., Smith, J.R., King, D.W., Meador, K.J., Park, Y.D., Loring, D.W., Clifton, G.L., Baumgartner, J.E., Tomas, A.B., Constantinou, J. E.C., Papanicolaou, A.C., 1999. A comparison of magnetoencephalography, MRI and V-EEG in patients evaluated for epilepsy surgery. *Epilepsia* 40, 931–941.
- Worrell, G.A., Lagerlund, T.D., Sharbrough, F.W., Brinkmann, B.H., Busacker, N.E., Cicora, K.M., O'Brien, T.J., 2000. Localization of the epileptic focus by low-resolution electromagnetic tomography in patients with a lesion demonstrated by MRI. *Brain Topography* 12, 273–282.
- Wyllie, E., Lüders, H.O., Morris, H.H.R., Lesser, R.P., Dinner, D.S., Rothner, A.D., Erenberg, G., Cruse, R., Friedman, D., Hahn, J., 1988. Subdural electrodes in the evaluation for epilepsy surgery in children and adults. *Neuropediatrics* 19, 80–86.
- Xu, X.L., Xu, B., He, B., 2004. An alternative subspace approach to EEG dipole source localization. *Physics in Medicine and Biology* 49, 327–343.
- Yoshida, F., Morioka, T., Hashiguchi, K., Miyagi, Y., Nagata, S., Oshshio, M., Sasaki, T., 2007. Display of the epileptogenic zone on the frontal cortical surface using dynamic voltage topography of ictal electrocorticographic discharges. *Minimally Invasive Neurosurgery* 50, 37–42.
- Zhang, Y., van Drongelen, W., Kohrman, M., He, B., 2008. Three-dimensional brain current source reconstruction from intra-cranial ECoG recordings. *Neuroimage* 42, 683–695.
- Zooma, R., Yeh, H.S., Privitera, M.D., Gartner, M.H., 1995. Lesionectomy versus electrophysiologically guided resection for temporal lobe tumors manifesting with complex partial seizures. *Journal of Neurosurgery* 83, 231–236.